

Rule-Based Gillespie Simulation of Chemical Systems

Erika M. Herrera Machado^{1,2}, Jakob L. Andersen¹, Rolf Fagerberg¹, Christoph Flamm³, Daniel Merkle^{3,1}, and Peter F. Stadler^{4–9}

¹Department of Mathematics and Computer Science, University of Southern Denmark, Odense, Denmark
²{jlandersen,rolf,machado}@imada.sdu.dk

³Faculty of Mathematics and Computer Science, Friedrich Schiller University Jena, Jena, Germany

³Faculty of Technology, Bielefeld University, Bielefeld, Germany daniel.merkle@uni-bielefeld.de

⁴Department of Theoretical Chemistry, University of Vienna, Wien, Austria xtof@tbi.univie.ac.at

⁵Bioinformatics Group, Department of Computer Science & Interdisciplinary Center for Bioinformatics & School for Embedded and Composite Artificial Intelligence (SECAI), Leipzig University, Leipzig, Germany
studla@bioinf.uni-leipzig.de

⁶Max Planck Institute for Mathematics in the Sciences, Leipzig, Germany

⁷Facultad de Ciencias, Universidad National de Colombia, Bogotá, Colombia

⁸Center for non-coding RNA in Technology and Health, University of Copenhagen, Frederiksberg, Denmark

⁹Santa Fe Institute, Santa Fe, NM, USA

September 30, 2025

Abstract

The MØD computational framework implements rule-based generative chemistries as explicit transformations of graphs representing chemical structural formulae. Here, we expand MØD by a stochastic simulation module that simulates the time evolution of species concentrations using Gillespie’s well-known stochastic simulation algorithm (SSA). This module distinguishes itself among competing implementations of rule-based stochastic simulation engines by its flexible network expansion mechanism and its functionality for defining custom reaction rate functions. It enables direct sampling from actual reactions instead of rules. We present methodology and implementation details followed by examples which demonstrate the capabilities of the stochastic simulation engine.

1 Introduction

Mathematical and computational models of chemical and biochemical reaction networks are indispensable for understanding the behavior of these systems. The stochastic modeling of chemical kinetics has been explored since the 1940s [14, 24, 26]. While the classical ODE-based approach is suitable for many cases, it may not accurately represent the true time evolution of a system where discreteness and stochasticity are important [4, 20]. This is in particular the case for systems with very small particle counts, such as proteins in single cells, which are poorly modelled by real-valued concentrations [22, 25].

Given a set of reactions $\{R_1, \dots, R_M\}$, stochastic chemical kinetics is determined by the propensity function of each reaction, which can be interpreted as a (non-normalized) probability that reaction R_i will occur in the system in the next time interval $[t, t + dt]$. The reaction probabilities in turn determine the Chemical Master Equation (CME), a continuous-time Markov process whose state space comprises the particle counts of all chemical species. Although the CME can be solved analytically in principle, this is usually impractical. In particular for highly nonlinear chemical reactions, even numerical solutions can be unfeasible. This motivates the use of stochastic simulation algorithms to generate sample trajectories of the system’s discrete state over time.

Gillespie's stochastic simulation algorithm (SSA) [20–22] has become a standard way to simulate chemical and biochemical systems and serves as the basis for various stochastic simulation tools that generate trajectories of species concentrations.

In its original version, SSA assumes that the whole set of reactions and all possible molecular species are explicitly enumerated in advance, which can be unfeasible in many cases. For instance, in the field of biochemical reaction networks, many proteins have multiple sites where chemical processes can alter them. A simple heterodimer of two different proteins, each with eight modifiable sites, for instance, would result in 256 different states, requiring more than 65,000 equations [13].

SSA can also be adapted to handle essentially open-ended systems in cases where it is feasible to, at each time step, enumerate all possible reaction channels and compute their associated rate constant. This setting has been used frequently in models of RNA evolution with replication rates dependent on the secondary structures of the parent RNA and mutations introduced uniformly [18, 19]. A similar application is the simulation framework ALF for genome evolution [12]. In the latter, genomes in the population also interact via lateral gene transfer, i.e., an offspring of a given parent may also include a piece of DNA copied from another member of the population.

Rule-based modeling addresses the issue of advanced enumeration of the system in a more general manner by representing species as agents and interactions as rules that describe how a local pattern should be transformed [8, 9]. Since a single rule can represent a class of reactions, this avoids the need to enumerate all possible reactions between all possible species [13]. Iteratively applying the rules according to their propensities can automatically construct the reaction network as part of the simulation, thus facilitating open-ended systems. Several specialized simulation frameworks have been developed to support this modeling approach.

The literature on stochastic simulation software is extensive. Here, we focus specifically on rule-based tools. The most popular are those that can execute models written in the BioNetGen Language (BNGL), and in Kappa. The simulation engines Nfsim [30] for BioNetGen and KaSim [7] for Kappa are essentially rule-based versions of Gillespie's SSA. The common theme of these approaches is their focus on abstract agents characterized by sites that carry state information and encode distinct interaction capabilities. Through their sites, agents connect into *site graphs* serving as the (molecular) entities to which rules are applied. Rules correspondingly specify transformations for patterns of sites. Each simulation step comprises three parts: (i) calculation of the propensity for each rule based on the current molecular state; (ii) sampling of the rule to be applied and the time step to the next event; (iii) application of the selected rule and update of the population of agents [7, 23]. This scheme avoids the explicit construction of the reaction network since the decision on the rule application to be executed can be made directly from the propensities of all applicable rules.

Using the same principles several alternative simulation engines have been developed. RuleMonkey [11], like Nfsim, is a stochastic simulator for models written in BNGL. PISKaS [27] is a multiscale simulation tool able to perform stochastic simulations on distributed memory computing architectures. It expands the Kappa language by allowing the explicit declaration of interconnected compartments to simulate heterogeneous environments and different types of transport between compartments. SimSG [15] is a general-purpose tool for performing rule-based simulations using stochastic graph transformations on site graphs. It uses a priority queue to schedule the execution of rule-match pairs. SYNTAX [10] is a rule-based stochastic simulator for metabolic pathways, operating on rules describing the transfer of carbon atoms from reactants to products. Site graphs provide a level of abstraction that is well-suited to describe interactions between macromolecular entities such as DNA strands or proteins. Models of small molecule chemistry, however, require a very fine-grained level of resolution in which agents describe single atoms. This is necessary to account for the fact that chemical reactions reshuffle the atoms between molecules, and to enable

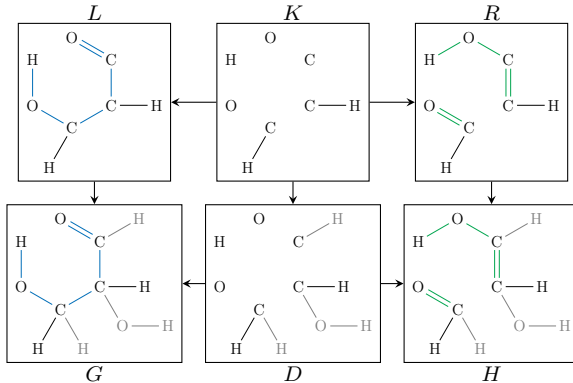


Figure 1: A Double-Pushout transformation representing a reverse aldol reaction. The rule is the top span $p = (L \leftarrow K \rightarrow R)$, which is applied to an input graph G . The transformation to the output H proceeds by first deleting the difference between L and K from G to obtain D , and then adding the difference between R and K to D to obtain the product graph H . The product in this case consists of multiple connected components, each representing a product molecule.

applications such as the design and analysis of stable isotope labeling experiments. Very little is gained by conceptualizing atoms as agents and molecules as site graphs. Rule-based stochastic simulations that operate directly on molecular graphs are much more natural for such applications.

We therefore describe here the implementation of a stochastic simulation module in MØD. This module combines a rigorous modeling approach for chemistry based on graph transformation rules with established stochastic simulation techniques. Atomistic explicitness, the ability for sampling the specific reaction to occur next in the system instead of sampling a rule, and a rich set of features from which to calculate reaction rates, are the main strengths offered by MØD’s stochastic simulation engine. This contribution is structured as follows: Section 2 introduces the software MØD. Section 3 reviews Gillespie’s stochastic simulation algorithm (SSA) and how reactions can be generated as needed. In Section 4, we outline the methodology used in our stochastic simulation engine, while Section 5 provides details on the implementation. Section 6 illustrates the application of the engine through various examples.

2 The MØD Software for Cheminformatics

In chemistry, molecules can be represented as undirected graphs where vertices correspond to atoms and edges represent bonds [32]. Labels associated with each vertex encode element type and charge, while labels on edges encode the specific bond type. In this representation, a chemical reaction can be modelled as a graph transformation rule [5, 28]. In essence, a graph transformation rule defines how a graph can be modified into a new one. A “seed” set of initial graphs together with a set of transformation rules is referred to as a graph grammar [29]. In the context of chemistry, rules are applied to a set of initial molecular graphs to yield new molecular graphs through the creation and destruction of bonds. By the Law of Conservation of Mass, vertices (i.e., atoms) can never be destroyed or created. MØD [2] is a software package that implements a chemically inspired graph transformation system based on the Double Pushout (DPO) formalism [29] for graph transformation. See Fig. 1 for an example of a DPO transformation rule and the corresponding derivation.

In contrast to the Single Pushout (SPO) approach, used for instance in Kappa, the DPO approach has no side effects during rule application, making the transformations invertible. This is more suitable for low-level chemistry, where individual atoms are tracked and chemical reactions

are in principle reversible. For more information on how the graph transformation engine is implemented in MØD, we refer to [2]. Although MØD implements DPO graph rewriting in full generality, it provides many features specifically designed for handling chemical data. It is also particularly effective for exploring and generating potential reaction networks by applying rules to the molecular inputs. It also includes algorithms for composing transformation rules, which can be used, for example, to abstract reaction mechanisms or entire trajectories into overall rules [3]. In addition to generic graph data, the software can load graphs from SMILES strings, and allows for visualizations of graphs, rules, and DPO diagrams, in a manner similar to how molecules are usually depicted in chemistry. MØD’s capability to model generic abstract graphs can be useful for applications in chemistry, e.g., when modeling chemistry where not all details are necessary, and parts of molecules can be merged into vertices with non-chemical labels.

3 Gillespie’s Stochastic Simulation Algorithm and *ad hoc* Reaction Generation

For completeness, we briefly recapitulate Gillespie’s stochastic simulation algorithm (SSA) [20] for a given state space. Gillespie defines the SSA as “a Monte Carlo procedure for numerically generating time trajectories of the molecular populations in exact accordance with the CME” [22]. The simulation generates successive states of a system, with each state being a vector specifying the molecular population of each species. Given such a state x , each reaction R_i has propensity $a_i(x)$, and the sum of all propensities is then denoted $a_{tot}(x)$. Each iteration of the simulation samples the next reaction to carry out according to the propensities, and the time to that next reaction from an exponential distribution with mean $1/a_{tot}(x)$. Specifically, two numbers r_1 and r_2 are drawn from a uniform distribution over $[0, 1]$, and the time to the next reaction is then calculated as $\tau = (-\ln r_1)/a_{tot}(x)$ and the index of the next reaction is calculated as the smallest integer j satisfying $\sum_{i=1}^j a_i(x) > r_2 \cdot a_{tot}(x)$. Each reaction R_j can be represented as a state change vector ν_j , and the next state is thus $x + \nu_j$.

In order to generalize this scheme, we note that in each iteration, only the reactions with non-zero propensity need to be known. Since the propensity of a reaction is zero if one of its reactants is not present in the population, any finite population only admits a finite set of applicable reactions, we can generate reactions as needed. We therefore arrive at Algorithm 1, where the extra step responsible for generating reactions on demand is marked in green. In traditional SSA, this step

```

Input:  $x_0$ ,  $t_0$ , and  $t_{max}$ 
 $i \leftarrow 0$ 
while  $t_i \leq t_{max}$  do
  Generate reactions originating in  $x_i$ 
  Update propensities  $a_j(x_i)$  for each event  $j$ , and  $a_{tot}(x_i)$ 
  Generate  $\tau$  and  $j$  and compute  $\nu_j$ 
   $t_{i+1} \leftarrow t_i + \tau$ ;  $x_{i+1} \leftarrow x_i + \nu_j$ 
  yield  $(x_{i+1}, t_{i+1}, j, \tau)$ 
   $i \leftarrow i + 1$ 
end

```

Algorithm 1: Generic version of Gillespie’s SSA.

is absent, as the reactions are given a priori. At the other end of the spectrum there are so-called

network free implementations, e.g., BioNetGen [17] and Kappa [7], where the reaction generation step is merged with the two subsequent steps of updating propensities and sampling reactions, such that rules and their matches in the current state are sampled according to the number of matches [31]. The rates are thus no longer defined per reaction, but are associated to rules. All reactions generated by the same rule therefore have the same rate.

4 Features of Stochastic Simulations in MØD

The approach we take here for implementation in MØD is that we explicitly generate reactions in a rule-based manner, but give the user the option to calculate a rate for each reaction through a custom rate function. Thus, the user retains full control over the reaction kinetics, which in particular can depend explicitly not only on the reactant molecules but also on the specific match of the reaction rule. To this end, the rate function has access to the graph structure of each molecule participating in a given reaction as well as which rule was used to generate the reaction. The rate calculation therefore can be as detailed as desired, from simply returning a fixed rate based on the rule to invoking quantum chemical tools. In programming terms, the rate function is implemented as a callback. Additional callbacks are supported in the simulation that provide the user with access to the information such as the current state and the iteration number.

A key feature of the graph transformation engine in MØD is its ability to not only enumerate all possible matches of a rule, but also make them available to the user. The rate callback therefore makes it possible to inspect different ways in which the left hand side of a rule can map onto the current set of molecules. This additional layer of control has at least two noteworthy uses as outline below.

4.1 Handling Symmetry and Effective Rule Activity

When multiple embeddings of the left-hand side of a rule are symmetrically equivalent, one may still choose to treat them as separate (each one contributes individually to the reaction propensity) or to treat them collectively (effectively “collapsing” them in a symmetry-aware way). In many rule-based approaches, such as Kappa, this is sometimes addressed by distinguishing between

1. non-deterministic rules that consider all symmetric embeddings to be just one “event”,
2. locally deterministic rules that treat each embedding as distinct unless the resulting outcomes are truly identical, or
3. ignoring symmetry entirely and counting all embeddings as distinct.

The possibility of explicitly enumerating all embeddings in MØD gives users the freedom to decide how symmetries should factor into their effective reaction rates. For instance, a user may wish to divide the total propensity of a reaction by the number of symmetric embeddings or, conversely, keep them all separate so that each embedding contributes fully to the rule’s activity. The precise choice depends on how the user interprets a rule application.

4.2 Atom Tracing and Embedding-Specific Events

In addition, having full access to each embedding can be crucial for atom tracing in simulations, such as those motivated by stable-isotope labeling experiments. In these settings, the location of a particular atom (e.g., a labelled carbon) might follow different trajectories depending on which

embedding is selected when the reaction occurs. Because MØD can distinguish between all possible ways of applying a rule, a callback can incorporate any external logic needed to pick a particular embedding or weigh them differently. As the result of the simulation is a trace of reactions, again with full access to molecular structures, so this isotope tracing can also be deferred to a post-processing step. This capability, while not the focus of the present work, underscores that the simulation engine can track individual atoms throughout the reaction network, providing a powerful extension for research that relies on identifying the fate of specific atoms in chemical or biochemical pathways.

5 Implementation

Applying graph transformation rules in every step of the simulation can slow down the algorithm significantly. Our implementation therefore employs several caching mechanisms. First, it leverages the strategy framework described in [1] which controls rule application with the help of a pair of sets of graphs: The universe \mathcal{U} comprises all molecular graphs that are available for transformation, and the distinguished subset $\mathcal{S} \subseteq \mathcal{U}$ which identifies the part of the universe that must participate in every reaction to be generated. Each reaction generated by a rule p corresponds to a proper direct derivation $G \xrightarrow{p} H$, where the graph G can be broken into a multiset of graphs corresponding to its connected components $\mathcal{G} = \{g_1, g_2, \dots, g_k\}$. Given a subset-universe pair $(\mathcal{U}, \mathcal{S})$ the framework will generate all direct derivations with $\mathcal{G} \subseteq \mathcal{U}$ and $\mathcal{G} \cap \mathcal{S}$.

This distinction of \mathcal{U} and \mathcal{S} provides a structured way to store newly derived molecules. In each simulation step, this makes it possible to limit the generation of reactions to those that involve a novel substrate. For a new state x_{i+1} based on state x_i , the universe \mathcal{U} is defined as all molecules with non-zero count in x_{i+1} and the subset \mathcal{S} is defined as all molecules that have count zero in x_i but non-zero in x_{i+1} . Note that if \mathcal{S} is empty, then no new reactions are generated. For the initial iteration we simply use $\mathcal{S} = \mathcal{U}$. MØD will cache all molecules and reactions generated, and thus, by induction, all relevant reactions will be available for the SSA in each iteration. In particular, if iteration i starts with state x_i with support \mathcal{U}_i , and a subsequent iteration i' has support $\mathcal{U}_{i'} \subseteq \mathcal{U}_i$, then no reactions need to be generated since they already have been calculated and cached. The implementation therefore caches each \mathcal{U}_i .

Importantly, these caching mechanisms only serve to speed up the algorithm, and thus if a user notices that memory usage becomes large (for example, in complex systems that expand into a large number of intermediate states), there is a straightforward option to “restart” the reaction generation by clearing the caches. Any subsequent iterations again generate new reactions and store them in fresh caches. This gives users direct control over balancing performance improvements from reusing reaction generation against memory constraints that can arise from storing large amounts of state information.

Under the hood, the core of the strategy system, the actual computation of graph embeddings, and the reaction data structures, are implemented in C++. The morphism algorithms that search for valid embeddings of the left-hand side of a rule in a molecular graph are thus executed efficiently. User-defined rate functions, which may depend on the number of embeddings or on specific topological properties of the molecules, can be provided in a Python-based interface, allowing flexible customization. By switching to custom or compiled callbacks if needed, performance can be optimized further in time-critical scenarios.

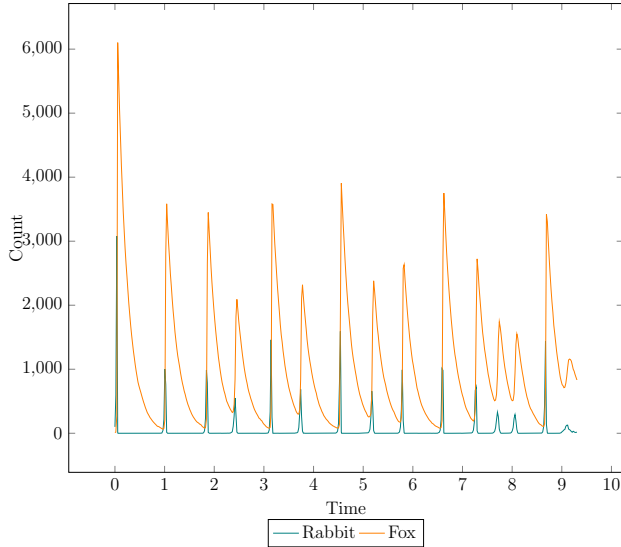


Figure 2: Oscillatory behavior of a Lotka-Volterra system using input and output flow.

6 Experiments

This chapter aims to show the practical applicability of the stochastic simulation module of MØD through a series of use cases.

6.1 Example 1: Lotka-Volterra System

In our initial example, we aim to illustrate how we can model population dynamics in MØD, specifically the well-known Lotka-Volterra predator-prey system, where foxes (Z) and rabbits (Y) interact. The dynamics can be captured through the following reactions:

```

replication_rabbits: Y → 2Y
replication_foxes: Y + Z → 2Z
growth_rabbits: Ø → Y
death_rabbits: Y → Ø
death_foxes: Z → Ø

```

The reaction rate callback will assign a constant rate of 100 to *replication_rabbits*, and a rate of 0.1 to *replication_foxes*. For the growth and death reactions, we employ the input and output rate callbacks: a constant input flow of 5 only for Y ; and an output flow of 5 for both species Y and Z . This way we open the system. Regarding initial concentrations we define $[Y] = 100$ and $[Z] = 10$. We let the simulation run until reaching 150,000 iterations. As shown in Figure 2, the resulting concentration evolution shows expected oscillatory behavior, characteristic of the Lotka-Volterra system. This confirms the model's capacity to represent predator-prey dynamics accurately within an open system.

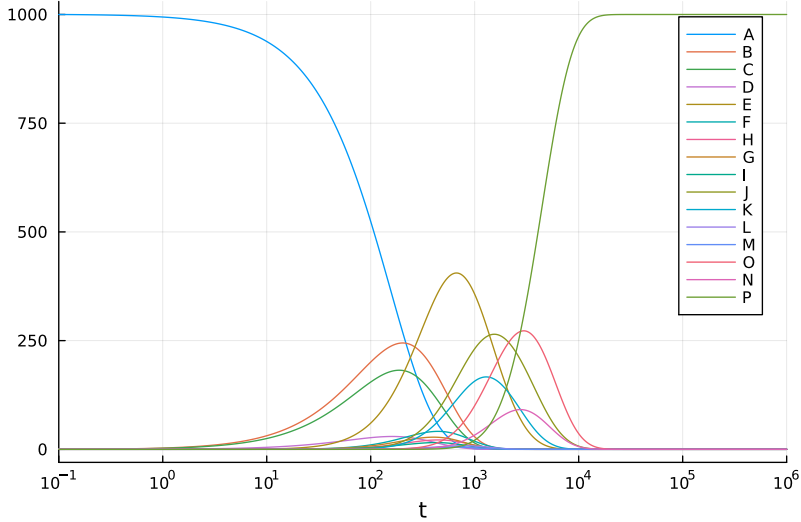


Figure 3: ODE-based degradation dynamics of atrazine in soil. As initial parameters, we have set a concentration value of 1000 for atrazine (molecule A), and a simulation time of 10^6 .

6.2 Example 2: Degradation of Atrazine

Our second example is a degradation process from atrazine to cyanuric acid. The degradation of such s-triazine herbicides under anaerobic conditions in soil can be described by only two major reaction types [16]:

- (1) Hydrolysis ($R-X \xrightarrow{H_2O} R-OH+HX$, where $X = Cl, NH_2$)
- (2) Reductive dealkylation ($R-NH-R' \xrightarrow{H_2} R-NH_2+HR'$, where R' is a C_1-C_4 alkyl-moiety such as ethyl, or iso-propyl).

These two reactions induce a reaction network transforming atrazine to cyanuric acid. To simulate the degradation dynamics we will use the rate constants from [16]:

$$\begin{aligned} k_{hydrolysis} &= 5.00 \times 10^{-9} s^{-1} \\ k_{de-ethylation} &= 3.32 \times 10^{-8} s^{-1} \\ k_{de-isopropylation} &= 2.65 \times 10^{-8} s^{-1} \end{aligned}$$

We first focus on the degradation network of atrazine in soil, which can be seen in Figure 7 in the Appendix. The possible chemical species were named by single characters (A–P), from atrazine (molecule A) to cyanuric acid (molecule P). To explore the system’s dynamics in a deterministic fashion, we can specify the set of ODEs using Julia [6]. The detailed definition of the reaction network is also included in the Appendix. Figure 3 shows the evolution of species concentrations.

The next experiment consists of replicating the deterministic evolution of species concentration using the stochastic simulation module of MØD. By comparing the behavior observed in the stochastic simulation against the ODE-based results, we aim to illustrate the stochastic engine’s correctness and consistency. We will start by modeling the closed system—no input or output flows occur.

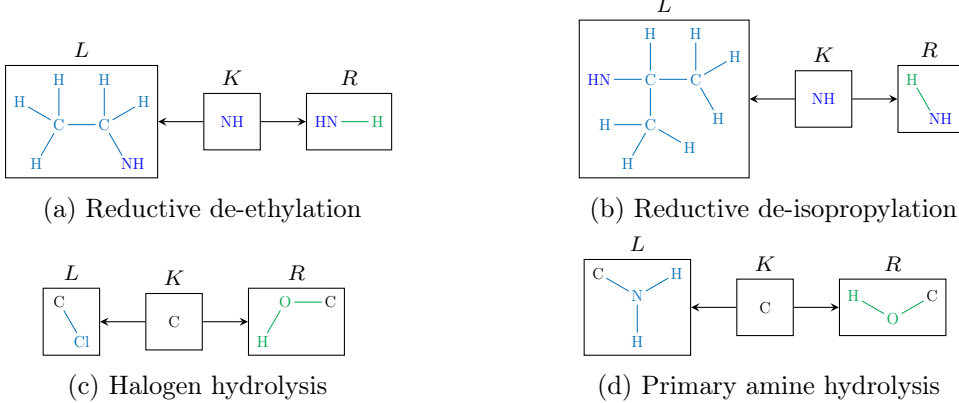


Figure 4: Graph transformation rules for the degradation of atrazine.

As previously mentioned, a graph grammar specifies the initial molecular graphs and the graph transformation rules that will be used to expand the chemical network when needed. For this example, however, we have defined all possible molecules in the system beforehand. As for the reaction rules, Figure 4 depicts the four rules that represent the necessary intramolecular bond relabeling.

MØD’s stochastic simulation module offers the possibility of defining different callbacks for sampling the next reaction in the system. We refer to this as reaction rate callback. The drawing function determines the reactivity of each reaction by applying the Law of Mass Action with the rates defined in the callback. Additionally, rates for both input and output flows to and from the chemical system can be specified. The input rate refers to the rate for pseudo-reactions that create molecules, while the output rate is the equivalent for destroying molecules. Both rates can be defined as either a callback or a constant value.

For our current system, we define the reaction rate callback by assigning rate constants to each of the four rules. Next, we set up the simulator by specifying the initial compounds and their concentrations. We can retrieve and analyze a representation of a trace of events from the simulation. The resulting simulated dynamics can be visualized in Figure 5. Notice how both plots reflect the same underlying dynamics through their matching shapes.

To continue showcasing the functionalities of the stochastic simulation engine, we open the system. To this end, we define the input rate of molecule A and the output rate of molecule P:

$$k_{inflow_A} = 4.00 \times 10^{-6} s^{-1}$$

$$k_{outflow_P} = 1.00 \times 10^{-8} s^{-1}$$

This results in a novel non-equilibrium steady state (NESS), where intermediate species coexist with molecule P. The conservation relation implied by mass conservation is lost in the open system.

6.3 Example 3: Conditional Callbacks

The following is a simple example intended to demonstrate another use of the reaction rate callbacks employing conditionals and molecular count checks.

Given a simple assembly system of molecules denoted A and B:

$$binding: \quad A + B \rightarrow AB$$

$$unbinding: \quad AB \rightarrow A + B$$

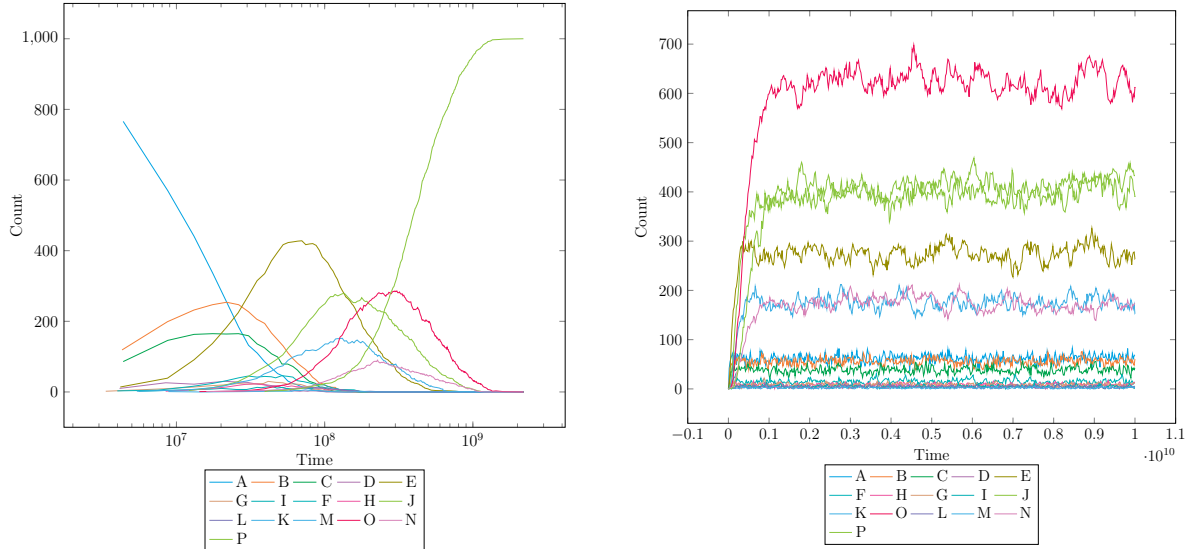


Figure 5: Time evolution of the stochastic simulation of the atrazine degradation. L.h.s.: Closed system. Initial concentration of atrazine (molecule A) is set to 1000. The simulation time is unbounded. R.h.s.: Open system.

We set the initial concentrations to $[A] = 100$ and $[B] = 500$ molecules. Regarding the reaction rate callback, the *binding* rule will have a rate constant of 0.01. For the *unbinding* rule, the rate constant will be 1 if $[A] > 200$; and 0.01 otherwise—balancing the rates of creation and destruction of bonds between A and B . Additionally, the system will have an input flow of A that we set to 5 while $[A] < 200$, producing a rapid increase; and to 0.01 otherwise.

We can visualize the resulting evolution of concentrations in Figure 6. We observe an initial decay in the concentration of B , as this molecule is in fixed amounts and it's being used to produce AB . Similarly, A is consumed very quickly at the beginning. When almost all B molecules are consumed, the rate of production of AB stabilizes close to 500 copies, around $t = 80$. At this point, the *binding* and *unbinding* rules are less reactive, and we can observe a rapid increase in the concentration of A . By design, when $[A] \geq 200$, at approximately $t = 125$, the input flow of A is reduced significantly, and the *unbinding* reaction will kinetically dominate over the *binding* one, resulting in equilibrium for all the species.

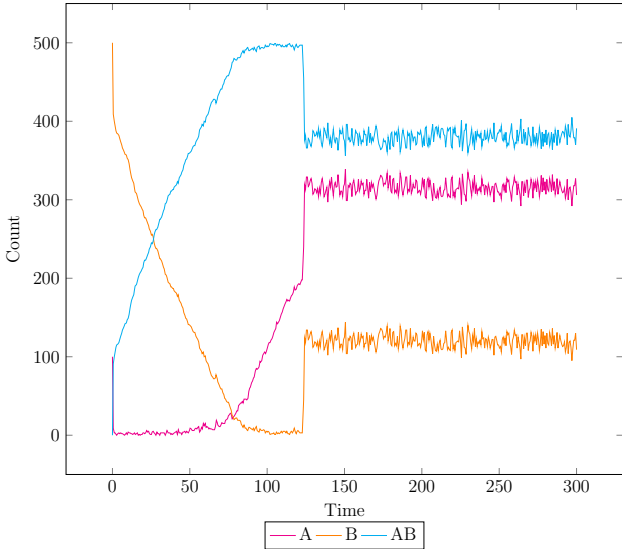


Figure 6: A stochastic simulation of a toy assembly system with conditional rates and input flow of A.

This example illustrates how reaction rate callbacks provide flexibility in controlling simulation behavior in response to real-time changes in molecular concentrations. By dynamically adjusting reaction rates based on conditions, callbacks enable complex and context-dependent dynamics, making them a powerful tool for modeling chemical systems.

References

- [1] Jakob L Andersen, Christoph Flamm, Daniel Merkle, and Peter F Stadler. Generic strategies for chemical space exploration. *International journal of computational biology and drug design*, 7(2-3):225–258, 2014.
- [2] Jakob L Andersen, Christoph Flamm, Daniel Merkle, and Peter F Stadler. A software package for chemically inspired graph transformation. In *Graph Transformation: 9th International Conference, ICGT 2016, in Memory of Hartmut Ehrig, Held as Part of STAF 2016, Vienna, Austria, July 5-6, 2016, Proceedings 9*, pages 73–88. Springer, 2016.
- [3] Jakob Lykke Andersen, Christoph Flamm, Daniel Merkle, and Peter F Stadler. 50 shades of rule composition: From chemical reactions to higher levels of abstraction. In *Formal Methods in Macro-Biology: First International Conference, FMMB 2014, Nouméa, New Caledonia, September 22-24, 2014. Proceedings 1*, pages 117–135. Springer, 2014.
- [4] Anthony F Bartholomay. Stochastic models for chemical reactions: I. theory of the unimolecular reaction process. *The bulletin of mathematical biophysics*, 20:175–190, 1958.
- [5] Gil Benkő, Christoph Flamm, and Peter F Stadler. A graph-based toy model of chemistry. *Journal of Chemical Information and Computer Sciences*, 43(4):1085–1093, 2003.
- [6] Jeff Bezanson, Alan Edelman, Stefan Karpinski, and Viral B Shah. Julia: A fresh approach to numerical computing. *SIAM review*, 59(1):65–98, 2017.

[7] Pierre Boutillier, Mutaamba Maasha, Xing Li, Héctor F Medina-Abarca, Jean Krivine, Jérôme Feret, Ioana Cristescu, Angus G Forbes, and Walter Fontana. The kappa platform for rule-based modeling. *Bioinformatics*, 34(13):i583–i592, 2018.

[8] Lily A Chylek, Leonard A Harris, James R Faeder, and William S Hlavacek. Modeling for (physical) biologists: an introduction to the rule-based approach. *Physical biology*, 12(4):045007, 2015.

[9] Lily A Chylek, Leonard A Harris, Chang-Shung Tung, James R Faeder, Carlos F Lopez, and William S Hlavacek. Rule-based modeling: a computational approach for studying biomolecular site dynamics in cell signaling systems. *Wiley Interdisciplinary Reviews: Systems Biology and Medicine*, 6(1):13–36, 2014.

[10] David M Cohen and Richard N Bergman. Syntax: a rule-based stochastic simulation of the time-varying concentrations of positional isotopomers of metabolic intermediates. *Computers and Biomedical Research*, 27(2):130–147, 1994.

[11] Joshua Colvin, Michael I Monine, Ryan N Gutenkunst, William S Hlavacek, Daniel D Von Hoff, and Richard G Posner. Rulemonkey: software for stochastic simulation of rule-based models. *BMC bioinformatics*, 11:1–14, 2010.

[12] Daniel A. Dalquen, Maria Anisimova, Gaston H. Gonnet, and Christophe Dessimoz. ALF – A simulation framework for genome evolution. *Molecular Biology and Evolution*, 29:1115–1123, 2012.

[13] Vincent Danos, Jérôme Feret, Walter Fontana, Russell Harmer, and Jean Krivine. Rule-based modelling of cellular signalling. In *International conference on concurrency theory*, pages 17–41. Springer, 2007.

[14] Max Delbrück. Statistical fluctuations in autocatalytic reactions. *The journal of chemical physics*, 8(1):120–124, 1940.

[15] Sebastian Ehmes, Lars Fritzsche, and Andy Schürr. Simsg: Rule-based simulation using stochastic graph transformation. *J. Object Technol.*, 18(3):1–1, 2019.

[16] Larry E Erickson, Kyung Hee Lee, and Darrell D Sumner. react. *Critical Reviews in Environmental Science and Technology*, 19(1):1–14, 1989.

[17] James R Faeder, Michael L Blinov, and William S Hlavacek. Rule-based modeling of biochemical systems with bionetgen. *Systems biology*, pages 113–167, 2009.

[18] Walter Fontana, Wolfgang Schnabl, and Peter Schuster. Physical aspects of evolutionary optimization and adaptation. *Phys. Rev. A*, 40:3301–3321, 1989.

[19] Walter Fontana and Peter Schuster. A computer model of evolutionary optimization. *Biophys. Chem.*, 26(2-3):123–147, 1987.

[20] Daniel T Gillespie. A general method for numerically simulating the stochastic time evolution of coupled chemical reactions. *Journal of computational physics*, 22(4):403–434, 1976.

[21] Daniel T Gillespie. Exact stochastic simulation of coupled chemical reactions. *The journal of physical chemistry*, 81(25):2340–2361, 1977.

[22] Daniel T Gillespie. Stochastic simulation of chemical kinetics. *Annu. Rev. Phys. Chem.*, 58(1):35–55, 2007.

[23] Leonard A Harris, Justin S Hogg, José-Juan Tapia, John AP Sekar, Sanjana Gupta, Ilya Korsunsky, Arshi Arora, Dipak Barua, Robert P Sheehan, and James R Faeder. Bionetgen 2.2: advances in rule-based modeling. *Bioinformatics*, 32(21):3366–3368, 2016.

[24] Hendrik Anthony Kramers. Brownian motion in a field of force and the diffusion model of chemical reactions. *physica*, 7(4):284–304, 1940.

[25] Donald A McQuarrie. Stochastic approach to chemical kinetics. *Journal of applied probability*, 4(3):413–478, 1967.

[26] Elliott W Montroll and Kurt E Shuler. The application of the theory of stochastic processes to chemical kinetics. *Advances in Chemical Physics*, pages 361–399, 1957.

[27] Tomas Perez-Acle, Ignacio Fuenzalida, Alberto JM Martin, Rodrigo Santibanez, Rodrigo Avaria, Alejandro Bernardin, Alvaro M Bustos, Daniel Garrido, Jonathan Dushoff, and James H Liu. Stochastic simulation of multiscale complex systems with piskas: A rule-based approach. *Biochemical and biophysical research communications*, 498(2):342–351, 2018.

[28] Francesc Rosselló and Gabriel Valiente. Analysis of metabolic pathways by graph transformation. In *International Conference on Graph Transformation*, pages 70–82. Springer, 2004.

[29] Grzegorz Rozenberg. *Handbook of graph grammars and computing by graph transformation*, volume 1. World scientific, Singapore, 1997.

[30] Michael W Sneddon, James R Faeder, and Thierry Emonet. Efficient modeling, simulation and coarse-graining of biological complexity with nfsim. *Nature methods*, 8(2):177–183, 2011.

[31] Ryan Suderman, Eshan D Mitra, Yen Ting Lin, Keesha E Erickson, Song Feng, and William S Hlavacek. Generalizing gillespie’s direct method to enable network-free simulations. *Bulletin of mathematical biology*, 81(8):2822–2848, 2019.

[32] James Joseph Sylvester. On an application of the new atomic theory to the graphical representation of the invariants and covariants of binary quantics, with three appendices. *American Journal of Mathematics*, 1(1):64–104, 1878.

A Atrazine degradation network

```

1 rn = @reaction_network Atrazine begin
2   @parameters k1 k2 k3
3   (k2, k3, k1), A --> (B, C, D)
4   (k3, k1, k1), B --> (E, F, H)
5   (k2, k1, k1), C --> (E, G, I)
6   (k2, k3), D --> (F, G)
7   (k1, k1), E --> (J, K)
8   (k3, k1), F --> (J, L)
9   (k2, k1), G --> (J, M)
10  (k2, k1), H --> (K, L)
11  (k2, k1), I --> (K, M)

```

```
12          k1, J --> 0
13  (k1, k1), K --> (N, 0)
14          k3, L --> 0
15          k2, M --> 0
16          k1, N --> P
17          k1, O --> P
18 end
```

Listing 1: Reaction Network for Atrazine Degradation ODE Model in Julia.

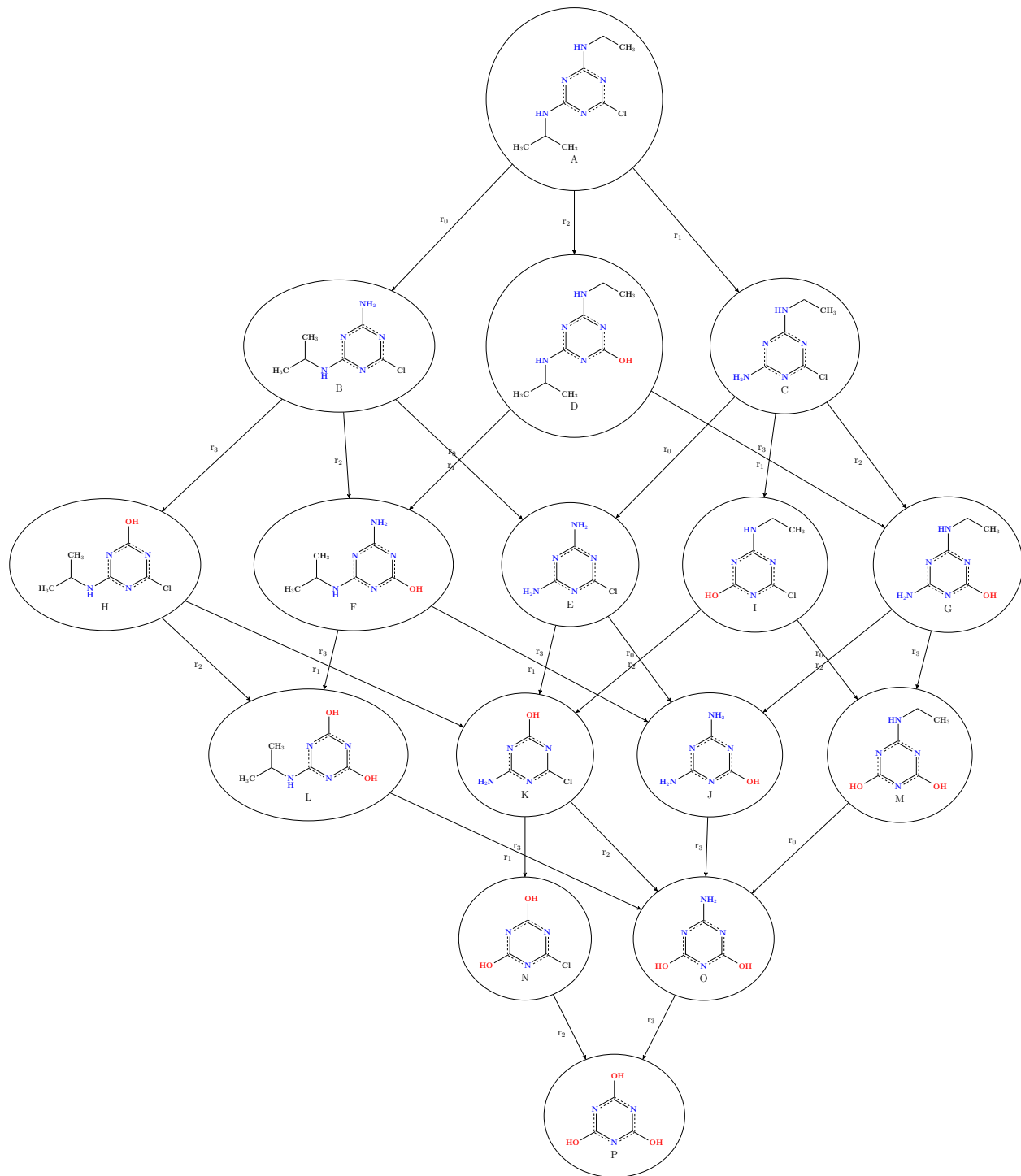


Figure 7: Atrazine degradation network depicting the pathway and intermediate products.